Available online at www.sciencedirect.com

ScienceDirect

Ceramics International 40 (2014) 4559–4565

CERAMICS INTERNATIONAL

www.elsevier.com/locate/ceramint

Synthesis and characterization of Ca–Sr–P coating on pure magnesium for biomedical application

Yanjin Lu[a,b,*], Lili Tan[b], Bingchun Zhang[b], Jinxin Lin[a], Ke Yang[b]

[a]Fujian Institute of Research on the Structure of Matter, Chinese Academy of Sciences, 155 Yangqiao Road West, Fuzhou 350002, China
[b]Institute of Metal Research, Chinese Academy of Sciences, 72 Wenhua Road, Shenyang, China

Received 23 May 2013; received in revised form 30 August 2013; accepted 30 August 2013
Available online 7 September 2013

Abstract

There are growing evidences that Sr-containing calcium phosphate biomaterials can promote better osteo-precursor cell attachment and proliferation than pure calcium phosphate biomaterials. In this study, attempts were made to fabricate two kinds of Sr-substituted calcium phosphate (Ca–Sr–P) coatings on pure magnesium in electrolyte solutions with differing amounts of $Sr(NO_3)_2$ for biomedical application. The surface microstructure, composition and chemistry of the coatings were characterized by Scanning Electron Microscope (SEM), Energy-dispersive X-ray Spectroscopy (EDS), and X-ray Diffractometer (XRD), respectively. In addition, electrochemical and immersion tests were performed to evaluate the corrosion resistance of the Ca–Sr–P coated magnesium in phosphate buffered saline solution (PBS).

Keywords: Strontium; Chemical deposition; Degradation; Bioactive coating; Magnesium

1. Introduction

In recent years, magnesium and its alloys have been widely studied for application in orthopedic implants due to their excellent properties, such as low toxicity, well biodegradation, attractive biocompatibility and excellent mechanical properties [1–3]. However, previous studies indicated that the fast degradation rate of magnesium implants in the physiological environment limits their clinical applications [4,5]. Avoiding this drawback, the degradation rate should be controlled to prevent early failure of implants from losing their mechanical integrities before the tissue healed [6]. Surface modification is a promising route to slow down the degradation rate in magnesium. Various surface modification technologies have been developed for magnesium to obtain protective coating, such as chemical deposition [7], biomimetic deposition [8], organic coating [9], sol–gel method [10], cathodic deposition [11,12], micro-arc oxidation [13], and pulsed laser deposition [14]. Calcium phosphate is used as a bone substitute in dentistry and orthopedics because of its excellent biocompatibility, non-toxicity, bioactivity and osseoconductivity [15]. Recently, calcium phosphate has also been applied as a coating for the purpose of modifying the surface of the magnesium and its alloys to promote the direct attachment to the surrounding hard tissue and to reduce the degradation rate [16]. For example, Song et al. [17] successfully applied calcium phosphate on biodegradable Mg–Zn alloy to improve its biocompatibility and promote osteointegration. It was also reported that an ion-beam assisted deposition HA coating on an AZ31 magnesium alloy can significantly decrease its degradation rate in a NaCl aqueous solution [18].

Strontium, as a natural bone-seeking trace element, can enhance osteoblast differentiation and inhibit osteoclast differentiation, and used in therapy that promotes bone mass and strength [19]. In vitro and in vivo studies have proven that strontium can increase bone formation, reduce bone resorption and improve bone mechanical strength in humanity [20,21]. Considering the beneficial effects of strontium in bone, strontium has been incorporated into apatite phases for biomedical implantation via various methods, due to the similarities shared with calcium in physical and chemical nature [22–24]. According to Gorustovich et al. [25], Sr-containing calcium phosphate

*corresponding author at: Fujian Institute of Research on the Structure of Matter, Chinese Academy of Sciences, 155 Yangqiao Road West, Fuzhou 350002. China. Tel./fax: +86 59183803765.
E-mail address: yjlu@fjirsm.ac.cn (Y. Lu).

0272-8842/$ - see front matter © 2013 Elsevier Ltd and Techna Group S.r.l. All rights reserved.
http://dx.doi.org/10.1016/j.ceramint.2013.08.132

ceramics can promote better osteoprecursor cell attachment and proliferation. Qiu et al. [26] also reported that Sr-substituted calcium phosphate could stimulate the proliferation and differentiation of osteoblastic cells in vitro. Furthermore, Strontium has also been introduced into the coatings on traditional metal for the application in biomaterials [27–29]. For example, Chung et al. [30] replaced calcium with differing percentages of strontium in order to fabricate Sr-substituted Hydroxycarbonate coatings to enhance the osseointegration of titanium implants by micro-arc oxidation. The work demonstrated that the Sr-substituted coatings could significantly inhibit the osteoclast differentiation when the content of strontium in Hydroxycarbonate coatings exceeds 38.9 wt%.

To date, notwithstanding many reports come out around Sr-containing calcium phosphate ceramics and cements for bone tissue repair in the last decade [25,31], few research work about the Ca–Sr–P coating on magnesium surface by chemical deposition has been carried out. Chemical deposition, compared with other methods, is an effective way to fabricate Ca–Sr–P coatings on magnesium. Therefore, the aim of this work is to develop Sr-containing calcium phosphate coatings on pure magnesium by chemical deposition with the purpose of slowing down the degradation rate of pure magnesium. Additionally, the investigation of how strontium content affects the surface microstructure, chemistry and magnesium degradation of resultant modified magnesium were also investigated.

2. Experiment

2.1. Preparation of samples

As-cast pure magnesium bar with a purity of 99.99% (0.0014Fe, 0.0001Ni, 0.0002Cu, 0.0016Si, 0.0004Al, 0.0004Mn and balance Mg, wt%) was cut into plates of 10 mm × 10 mm × 2 mm. These samples were ground with grit SiC papers to 1200 grit, then cleaned in acetone for 10 min, rinsed in distilled water and finally dried at room temperature. Then, the samples were immersed into two kinds of electrolyte solutions at 70 °C for 24 h. After the coating process, the samples were washed with deionized water to remove the residue of the electrolyte solutions. The chemical composition of these electrolyte solutions is listed in Table 1, in which they are denoted as CD-1 and CD-2, in accordance with the content of strontium in the electrolyte solution.

Table 1
The chemical composition of the electrolyte solutions (g/L).

Composition	$Ca(NO_3)_2 \cdot 4H_2O$	$Sr(NO_3)_2$	$NaH_2PO_4 \cdot 2H_2O$
CD-1	36	4	16
CD-2	28	12	16

2.2. Measurement of Sr-containing calcium phosphate coating

The morphologies of Sr-containing calcium phosphate coatings were characterized by a scanning electron microscope (SEM, Inspect F50) equipped with energy-dispersive X-ray spectroscopy (EDS). An X-ray diffractometer (XRD, D/MAX-2500PC) was used to identify the phase analysis on coatings. The XRD pattern was made with MDI Jade 5.0 software.

2.3. Electrochemical test

An electrochemical test was also conducted to evaluate the protective capacity of the coating on the magnesium substrate in the phosphate buffered saline (PBS) solution at 37 °C. A three-electrode cell was used for the electrochemical measurements. The counter electrode was made of platinum and a saturated calomel electrode (SCE) was used as the reference electrode. A sample with an exposed area of 1 cm^2 was taken as the working electrode. Before the test, all samples were immersed in the PBS solution for 30 min to obtain an electrochemical steady state. The polarization scan was started from an anodic region from 250 mV below open circuit potential at a constant voltage scan rate of 0.5 mV/s.

2.4. Immersion test

The further evolution of the corrosion resistance of the Ca–Sr–P coated magnesium was carried out through an immersion test in PBS solution. In order to examine the degradation behavior of the samples, the in vitro immersion test was performed in PBS solution. Each sample was soaked with the PBS solution kept in an airtight container at 37 °C in a carbon dioxide incubator. The ratio of sample area to solution volume was 1.25 cm^2/mL. The immersion solutions were refreshed every day to simulate the real in vivo condition. The morphologies of coatings after 14 days of immersion were observed on SEM.

3. Results

3.1. Microstructure and phase identification

The morphologies and element content of coatings are shown in Fig. 1(a–d.) Obviously, the two kinds of coating densely cover on the magnesium substrate without any defects after exposure to a $Sr(NO_3)_2$-containing electrolyte solution. It is clear to see that when the 4 g/L $Ca(NO_3)_2$ was replaced by $Sr(NO_3)_2$, only well-crystalline Sr-substituted calcium phosphate is found in the CD-1 coating as shown in Fig. 1(a–b.) But when the concentration of $Sr(NO_3)_2$ increased the situation is reversed as shown in Fig. 1c, a distinct change is observed in the structure of the CD-2 coating; at higher magnification (Fig. 1d) it shows two phases coexist on the CD-2 coating: the one presents well-crystalline structure (marked I), and the other presents poor-crystalline structure (marked II), indicating that strontium has a strong influence on the microstructure of the coatings.

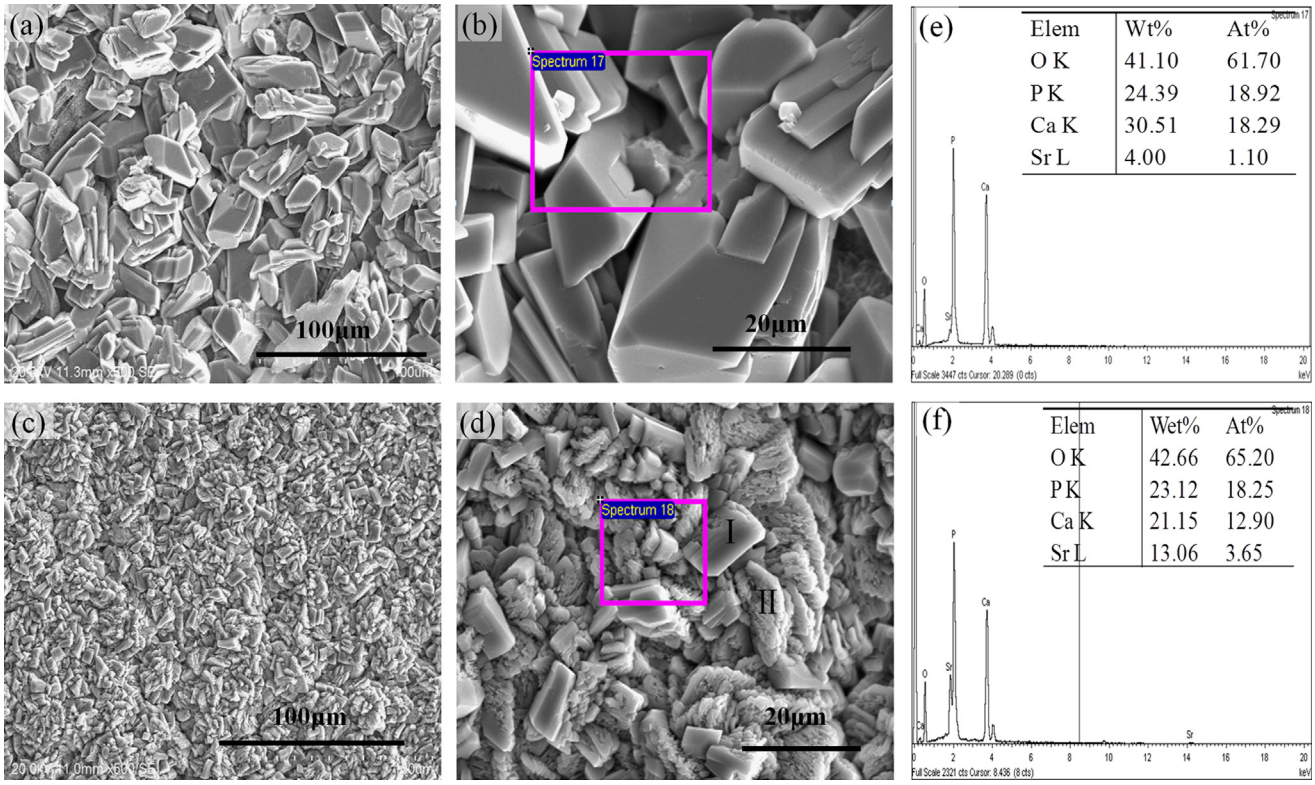

Fig. 1. SEM micrographs and EDS patterns of coatings: CD-1 coating (a), (b) and (e), CD-2 coating (c), (d) and (f).

Fig. 2(e–f) is the EDS patterns of the coatings. From the patterns of the designated area of the two kinds of coatings, it can be seen that the peaks of Sr are clearly observed. This demonstrates that strontium was successfully incorporated into the calcium phosphate. Moreover, the absence of the peak of Mg suggests Ca–Sr–P coatings densely cover on the magnesium substrate. Also, it is interesting to note from Table 2 that the atomic ratio of Sr in the poor-crystalline structure (marked II) is higher than that in the well-crystalline structure (marked I) in the CD-2 coating.

From the cross-section SEM micrographs shown in Fig. 2 (a–b), both the coatings are well integrated with the magnesium substrate. The average thicknesses of the CD-1 and CD-2 coatings are approximately 17.78 μm and 8.90 μm. Furthermore, an obvious decrease in thickness can also be observed as the concentration of strontium increase, indicating that the addition of strontium can inhibit the thickness of coating from growing. Apparently, the addition of strontium into the calcium phosphate can significantly affect the morphologies and the thickness of the coatings.

X-ray diffraction (XRD) patterns obtained from the two kinds of coatings are delineated in Fig. 3. Apart from the peaks of Mg, characteristic peaks of $Mg_3(PO_4)_2$, $CaPO_3(OH)$, $Ca_3(PO_4)_2$, $Ca_2Sr(PO_4)_2$ and $CaSr_9(PO_4)_6(OH)_2$ are also found in both of the XRD patterns. Compared with the CD-1 coating, the diffraction pattern of the CD-2 coating is slightly shifted to lower diffraction angles with the increase in the width of the X-ray line as an increasing amount of strontium was introduced. These results indicate that the incorporation of larger doses of strontium introduce more lattice distortions in the structure of calcium phosphate, because the ionic radius of strontium (113 pm) is appreciably larger than that of calcium (99 pm) [30,32,33]. Interestingly, even though the peaks of Mg are not revealed in the EDS analysis, $Mg_3(PO_4)_2$ was still detected in the coatings. It is probable that the $Mg_3(PO_4)_2$ phase might be covered under thick calcium phosphate coatings, which could not be detected by EDS.

3.2. Electrochemical test

Fig. 4 shows the polarization curves of magnesium with and without a coating in PBS solution at 37 °C. The corrosion current density (i_{corr}) and corrosion potential (E_{corr}) obtained from these curves are listed in Table 3. From the polarization curves, it is clear to see that the corrosion current density of pure magnesium quickly increases at the beginning of the anodic side. This suggests that the pure magnesium had undergone a severe corrosion attack in PBS solution [34]. After the pure magnesium was modified by chemical deposition treatment, the corrosion potential (E_{corr}) of the coated magnesium is shifted to significantly more noble potentials (more than 400 mV) relative to the pure magnesium. This great difference implies that the Ca–Sr–P coated magnesium has much lower corrosion rate and better corrosion resistance in PBS solution. Moreover, the corrosion current densities of the Ca–Sr–P coated magnesium are decreased by 2 orders of magnitude with respect to the pure magnesium, implying that the degradation rate of magnesium is indeed retarded by the

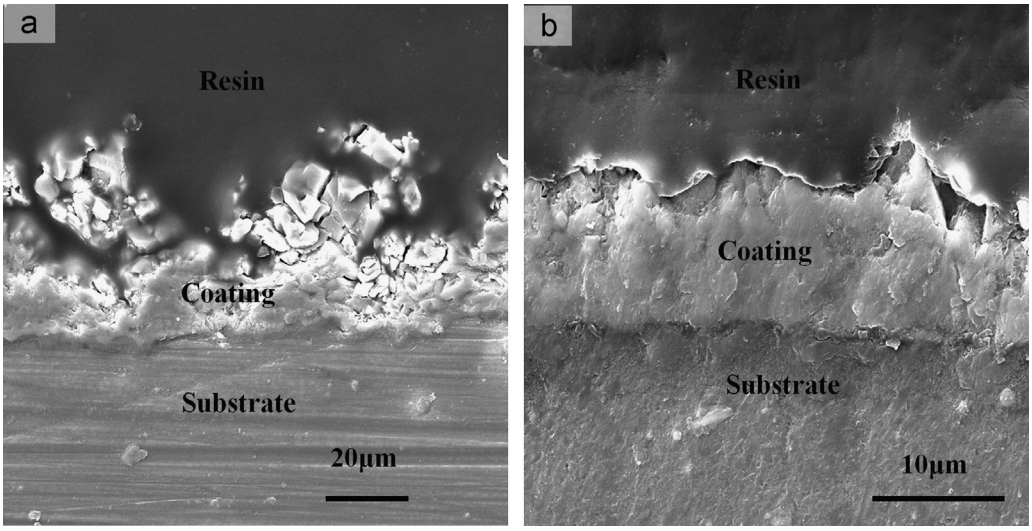

Fig. 2. The cross-section SEM micrograph of the coated magnesium: CD-1 coating (a), CD-2 coating (b).

Table 2
The EDS results of the designated points in Fig. 1(b).

Points	Elements (at%)			
	O K	PK	Ca K	SrL
I	56.09	22.56	17.45	3.90
II	62.54	19.53	10.40	7.53

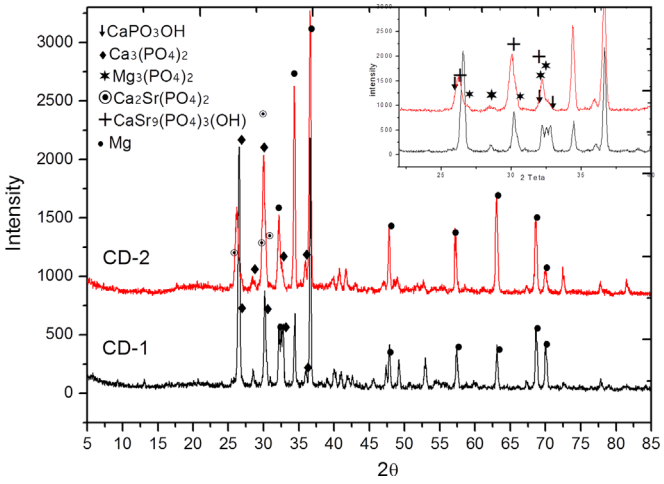

Fig. 3. XRD patterns of the coatings formed in different electrolyte solutions.

inhibition of hydrogen reduction. It should be noted that no obvious difference can be observed between the CD-1 and CD-2 groups in the polarization curves. This indicates that the two kinds of Ca–Sr–P coatings had a similar corrosion resistance performance at the initial stage. From the measured results it evidences that the corrosion resistance of magnesium substrate is considerably improved by the chemical deposition treatment in electrolyte solutions with the addition of $Sr(NO_3)_2$.

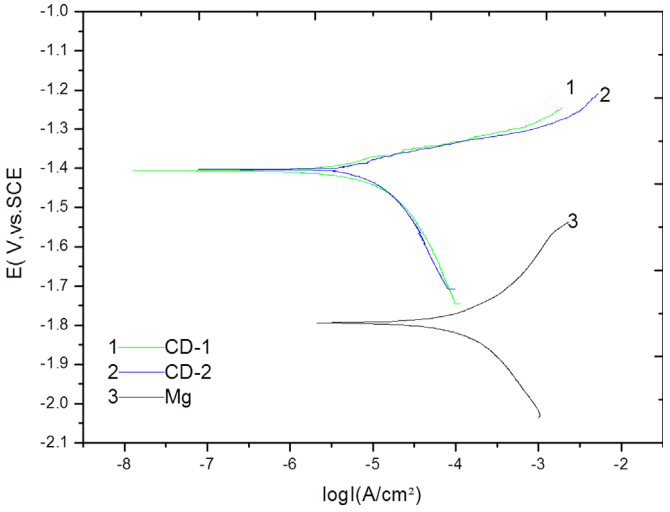

Fig. 4. Polarization curves of the magnesium with and without coating in PBS solution at 37 °C.

Table 3
The E_{corr} and i_{corr} of the magnesium with and without coating.

Samples	i_{corr} (A/cm^2)	E_{corr} (V)
Bare Mg	1.36E-4	−1.795
CD-1	3.75E-6	−1.395
CD-2	5.77E-6	−1.400

3.3. Immersion test

Generally, when magnesium is exposed to an aqueous solution the following reaction takes place: $Mg+2H_2O \rightarrow Mg^{2+}+2OH^-+H_2\uparrow$. As a consequence, the degradation of magnesium leads to an increase of the pH value in the surrounding area. In this study, the pH values for the PBS solution following immersion coated and uncoated magnesium were recorded, and the corresponding results are shown in

Fig. 5. It can be found that the pH values for the solutions immersed with Ca–Sr–P coated samples stay at lower levels during the immersion time in comparison with that of bare magnesium, suggesting the degradation rate of magnesium was markedly reduced due to the existence of the Ca–Sr–P coatings.

Additionally, an obvious variation of the pH curves between the two coated magnesium is observed. For the CD-1 group, the pH value increases rapidly in the initial period, and then gradually reaches a stable value after further immersion. Conversely, for the CD-2 group, the pH variation seems to fluctuate more and the average pH value is higher than that of the CD-1 group. This large difference could be attributed to the thickness and the dissolution of the coating. The further reason possibly due to more strontium replacement of the calcium affected the degree of crystallinity, thereby altered its solubility [35]. The pH measurement reveals that the Ca–Sr–P coatings can slow down the corrosion rate of magnesium, and the CD-1 group has certain advantages over the other group in the corrosion resistance.

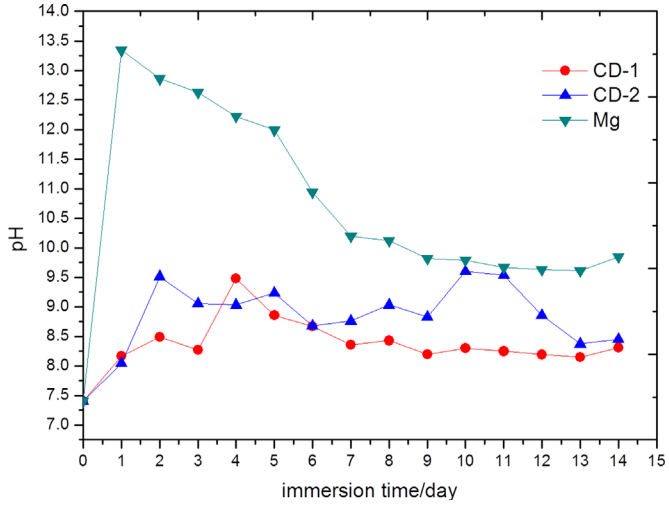

Fig. 5. Variation of pH value of PBS solutions containing magnesium samples with and without coatings.

Fig. 6(a–d) shows the SEM images of the coated magnesium after being immersed in the PBS solution at 37°C for 14 days. It seems that both magnesium substrates are still covered by dense coatings, indicating the coatings have a good protective effect from the PBS solution. As can be seen from Fig. 6a–b, in which the morphologies of the CD-1 crystals are shown, the crystals are more crystalline than that without immersion. The EDS pattern (Fig. 6e) of the framed area in Fig. 6(b) suggests that the peaks of Ca, P, O and Sr were detected but the peak Mg was absent. This can indirectly infer that Mg^{2+} did not incorporate into the Ca–Sr–P crystals during the immersion. The reason for this is probably the replacement of a small amount of strontium into the coating stabilized the crystals; consequently, the dissolution of the coating was drastically inhibited, as well as the release of the Mg^{2+} and OH^{-} ions. This coincides with the fairly stable pH value curve of the CD-1 group as observed in pH test. As regards the CD-2 coating, new bar-like crystals formed on the coating during the immersion, which is further confirmed by the EDS pattern in Fig. 6(f). It can be found from the EDS pattern that the main composition of the new bar-like crystals, as the arrow shows in Fig. 6(d), is Mg, O and P, but with no corresponding peak of Ca is detected. This implies that a mass of Mg^{2+} and OH^{-} ions released from the substrate, and reacted with phosphate

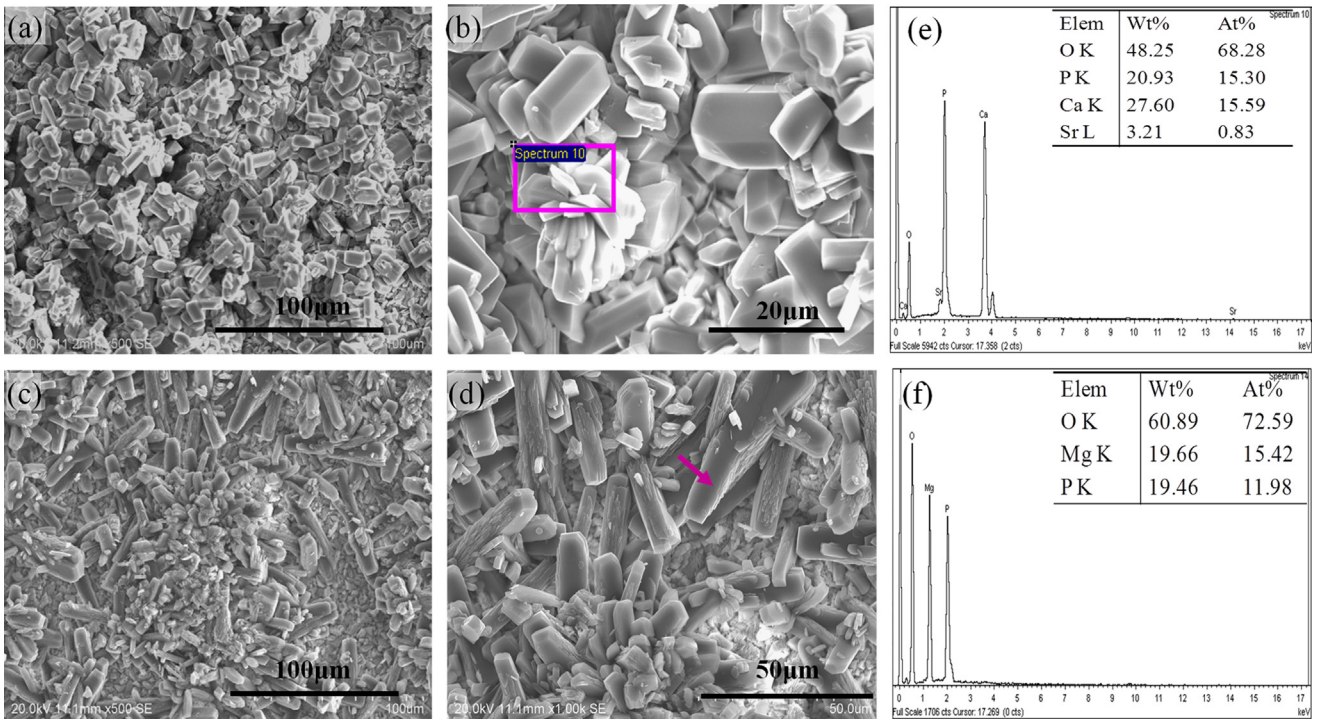

Fig. 6. SEM micrographs and EDS patterns of the coatings immersed in PBS for 14 days, CD-1 coating (a), (b) and (e); CD-2 coating (c), (d) and (f).

ions prior to calcium ions to form the magnesium phosphate at 37°C during the immersion process [36,37], which is also consistent with the fluctuation of the pH curve.

4. Discussion

In this study, the Ca–Sr–P coatings were fabricated on pure magnesium by chemical deposition. In view of the results of the electrochemical and immersion tests, the CD-1 and CD-2 coatings can significantly reduce the corrosion rate of pure magnesium. However, the CD-1 sample exhibits better corrosion resistance than the CD-2 sample. Generally, the corrosion resistance of coatings is governed by thickness and stability of phases [6,38]. Therefore, the thickness and the stability of phases were considered in this study to be the main factors to evaluate the corrosion resistance of Ca–Sr–P coatings. The pH test was conducted to investigate the long term degradation behavior of the magnesium, and approximately considered to be an evaluation of the Mg^{2+} and OH^- ion concentration of the immersion solution [38]. According to the pH curves, the pH values for immersion of CD-2 sample reaches a higher level than that of the CD-1 sample. As analyzed, on one hand, the thickness of coating could be used to explain the phenomenon. For higher Sr contents, the thickness of the CD-2 coating distinctly decreases in comparison with the CD-1 coating, as shown in Fig. 2. So it is easy for corrosion ions permeated to the CD-2 substrate, leading to a higher degradation rate. The repeated and sudden pH elevation can imply the existence of continuous pit corrosions in the CD-2 sample. Generally speaking, the thicker the coating is, the harder the corrosive ions penetrate through the substrate [39].

On the other hand, the stability of phases should be also responsible for the degradation rate of the substrate. Previous studies [32,40] have proven that when more incorporation of the strontium introduced into the structure of HA, the HA displayed greater solubility in physiological solution. In other word, the stability of the calcium phosphate will be changed with the increasing substitution of strontium. As can be seen from SEM images (Fig. 1b and d), at low strontium contents the calcium phosphate presents well crystallinity; whereas when calcium phosphate induced the incorporation of more strontium, the crystal size and crystallinity of Sr-substituted calcium phosphate of the CD-2 coating drops dramatically, which can be confirmed by the XRD patterns (Fig. 3). The XRD pattern of the CD-2 coating containing more strontium exhibits broader peaks, in line with a reduced degree of crystallinity or the presence of an amorphous phase [20,41]. Therefore, the poor-crystalline phases at relatively higher Sr contents may cause the CD-2 sample to have the rapid degradation as it can be deduced from higher pH value and the formation of Mg-composing bar-like crystals (Fig. 6d) during the immersion. In contrast, the phases of the CD-1 coating at low Sr contents exhibits well crystallinity (Fig. 1a-b), and displays better corrosion resistance property than that of the CD-2 coating. In brief, both the thickness and the stability of phases endow the CD-1 coating with the excellent corrosion resistance.

5. Conclusions

In this study, new composite coatings based on Sr-substituted calcium phosphate were fabricated in Sr-containing electrolyte solutions by chemical deposition for controlling the corrosion rate of magnesium. Results show strontium not only changed the microstructure of the coating, but also led to a decrease in the thickness of coating. On the other hand, the strontium can incorporate into calcium phosphate, and then the formed Sr-containing coatings could effectively protect the magnesium substrate from the degradation. In addition, the CD-1 coating had certain advantages over the CD-2 coating in corrosion resistance.

Acknowledgments

This work was financially supported by the National Natural Science Foundation of China (No. 30970715) and National Basic Research Program of China (No. 2012CB619101). We thank research assistant Peng Wan and Xiaoming Yu (IMR, CAS) for giving help and discussion on the experiments. We are also truly grateful to Stephanie Banks (University of Brighton), Minming Li (Purdue University) and Zaidong Li (University of Warwick) for their hard work on our manuscript.

References

[1] M. Haude, R. Erbel, P. Erne, S. Verheye, H. Degen, D. Böse, P. Vermeersch, I. Wijnbergen, N. Weissman, F. Prati, R. Waksman, J. Koolen, Safety and performance of the drug-eluting absorbable metal scaffold (DREAMS) in patients with de-novo coronary lesions: 12 month results of the prospective, multicentre, first-in-man BIOSOLVE-I trial, The Lancet 381 (9869) (2013) 836–844.

[2] M.P. Staiger, A.M. Pietak, J. Huadmai, G. Dias, Magnesium and its alloys as orthopedic biomaterials: a review, Biomaterials 27 (9) (2006) 1728–1734.

[3] F. Witte, J. Fischer, J. Nellesen, H.A. Crostack, V. Kaese, A. Pisch, F. Beckmann, H. Windhagen, In vitro and in vivo corrosion measurements of magnesium alloys, Biomaterials 27 (7) (2006) 1013–1018.

[4] N.T. Kirkland, J. Lespagnol, N. Birbilis, M.P. Staiger, A survey of bio-corrosion rates of magnesium alloys, Corrosion Science 52 (2) (2010) 287–291.

[5] F. Witte, F. Feyerabend, P. Maier, J. Fischer, M. Störmer, C. Blawert, W. Dietzel, N. Hort, Biodegradable magnesium–hydroxyapatite metal matrix composites MTT-assay, Biomaterials 28 (13) (2007) 2163–2174.

[6] J. Gan, L. Tan, K. Yang, Z. Hu, Q. Zhang, X. Fan, Y. Li, W. Li, Bioactive Ca–P coating with self-sealing structure on pure magnesium, Journal of Materials Science: Materials in Medicine 24 (4) (2013) 889–901.

[7] S.S. Singh, A. Roy, B. Lee, P.N. Kumta, Aqueous deposition of calcium phosphates and silicate substituted calcium phosphates on magnesium alloys, Materials Science and Engineering: B 176 (20) (2011) 1695–1702.

[8] S. Keim, J.G. Brunner, B. Fabry, S. Virtanen, Control of magnesium corrosion and biocompatibility with biomimetic coatings, Journal of Biomedical Materials Research Part B: Applied Biomaterials 96B (1) (2011) 84–90.

[9] C.H. Ye, Y.F. Zheng, S.Q. Wang, T.F. Xi, Y.D. Li, In vitro corrosion and biocompatibility study of phytic acid modified WE43 magnesium alloy, Applied Surface Science 258 (8) (2012) 3420–3427.

[10] J. Hu, C. Zhang, B. Cui, K. Bai, S. Guan, L. Wang, S. Zhu, In vitro degradation of AZ31 magnesium alloy coated with nano TiO_2 film by sol–gel method, Applied Surface Science 257 (2011) 8772–8777.

[11] P. Liu, X. Pan, W. Yang, K. Cai, Y. Chen, Al_2O_3–ZrO_2 ceramic coatings fabricated on WE43 magnesium alloy by cathodic plasma electrolytic deposition, Materials Letters 70 (2012) 16–18.
[12] C. Wen, S. Guan, L. Peng, C. Ren, X. Wang, Z. Hu, Characterization and degradation behavior of AZ31 alloy surface modified by bone-like hydroxyapatite for implant applications, Applied Surface Science 255 (13–14) (2009) 6433–6438.
[13] J.H. Gao, S.K. Guan, J. Chen, L.G. Wang, S.J. Zhu, J.H. Hu, Z.W. Ren, Fabrication and characterization of rod-like nano-hydroxyapatite on MAO coating supported on Mg–Zn–Ca alloy, Applied Surface Science 257 (6) (2011) 2231–2237.
[14] T.M. Yue, H. Xie, X. Lin, H.O. Yang, Microstructure development in laser forming of zirconium coatings on AZ91D magnesium alloy substrates, Journal of Alloys and Compounds 512 (1) (2012) 328–331.
[15] S. Shadanbaz, G.J. Dias, Calcium phosphate coatings on magnesium alloys for biomedical applications: A review, Acta Biomaterialia 8 (1) (2012) 20–30.
[16] L. Xu, F. Pan, G. Yu, L. Yang, E. Zhang, K. Yang, In vitro and in vivo evaluation of the surface bioactivity of a calcium phosphate coated magnesium alloy, Biomaterials 30 (8) (2009) 1512–1523.
[17] Y. Song, S. Zhang, J. Li, C. Zhao, X. Zhang, Electrodeposition of Ca–P coatings on biodegradable Mg alloy: In vitro biomineralization behavior, Acta Biomaterialia 6 (5) (2010) 1736–1742.
[18] J.X. Yang, Y.P. Jiao, F.Z. Cui, I.-S. Lee, Q.S. Yin, Y. Zhang, Modification of degradation behavior of magnesium alloy by IBAD coating of calcium phosphate, Surface and Coatings Technology 202 (22–23) (2008) 5733–5736.
[19] Y.C. Fredholm, N. Karpukhina, R.V. Law, R.G. Hill, Strontium containing bioactive glasses: Glass structure and physical properties, Journal of Non-Crystalline Solids 356 (44–49) (2010) 2546–2551.
[20] Z.Y. Li, W.M. Lam, C. Yang, B. Xu, G.X. Ni, S.A. Abbah, K.M.C. Cheung, K.D.K. Luk, W.W. Lu, Chemical composition, crystal size and lattice structural changes after incorporation of strontium into biomimetic apatite, Biomaterials 28 (7) (2007) 1452–1460.
[21] S. Pors Nielsen, The biological role of strontium, Bone 35 (3) (2004) 583–588.
[22] D. Guo, K. Xu, X. Zhao, Y. Han, Development of a strontium-containing hydroxyapatite bone cement, Biomaterials 26 (19) (2005) 4073–4083.
[23] S. Pina, P.M. Torres, F. Goetz-Neunhoeffer, J. Neubauer, J.M.F. Ferreira, Newly developed Sr-substituted α-TCP bone cements, Acta Biomaterialia 6 (3) (2010) 928–935.
[24] G.X. Ni, W.W. Lu, K.Y. Chiu, Z.Y. Li, D.Y.T. Fong, K.D.K. Luk, Strontium-containing hydroxyapatite (Sr-HA) bioactive cement for primary hip replacement: An in vivo study, Journal of Biomedical Materials Research Part B: Applied Biomaterials 77B (2) (2006) 409–415.
[25] A.A. Gorustovich, T. Steimetz, R.L. Cabrini, J.M. Porto Lopez, Osteoconductivity of strontium-doped bioactive glass particles: A histomorphometric study in rats, Journal of Biomedical Materials Research Part A 92A (1) (2010) 232–237.
[26] K. Qiu, X.J. Zhao, C.X. Wan, C.S. Zhao, Y.W. Chen, Effect of strontium ions on the growth of ROS17/2.8 cells on porous calcium polyphosphate scaffolds, Biomaterials 27 (8) (2006) 1277–1286.
[27] W. Xia, C. Lindahl, J. Lausmaa, P. Borchardt, A. Ballo, P. Thomsen, H. Engqvist, Biomineralized strontium-substituted apatite/titanium dioxide coating on titanium surfaces, Acta Biomaterialia 6 (4) (2010) 1591–1600.
[28] K. Nan, T. Wu, J. Chen, S. Jiang, Y. Huang, G. Pei, Strontium doped hydroxyapatite film formed by micro-arc oxidation, Materials Science and Engineering C 29 (5) (2009) 1554–1558.
[29] D. Gopi, S. Ramya, D. Rajeswari, L. Kavitha, Corrosion protection performance of porous strontium hydroxyapatite coating on polypyrrole coated 316L stainless steel, Colloids and Surfaces B: Biointerfaces 107 (2013) 130–136.
[30] C.-J. Chung, H.-Y. Long, Systematic strontium substitution in hydroxyapatite coatings on titanium via micro-arc treatment and their osteoblast/osteoclast responses, Acta Biomaterialia 7 (11) (2011) 4081–4087.
[31] G.X. Ni, W.W. Lu, B. Xu, K.Y. Chiu, C. Yang, Z.Y. Li, W.M. Lam, K.D.K. Luk, Interfacial behaviour of strontium-containing hydroxyapatite cement with cancellous and cortical bone, Biomaterials 27 (29) (2006) 5127–5133.
[32] W.M. Lam, H.B. Pan, Z.Y. Li, C. Yang, W.K. Chan, C.T. Wong, K.D.K. Luk, W.W. Lu, Strontium-substituted calcium phosphates prepared by hydrothermal method under linoleic acid-ethanol solution, Ceramics International 36 (2) (2010) 683–688.
[33] X. Wang, J. Ye, Variation of crystal structure of hydroxyapatite in calcium phosphate cement by the substitution of strontium ions, Journal of Materials Science: Materials in Medicine 19 (3) (2007) 1183–1186.
[34] P. Wan, J. Wu, L. Tan, B. Zhang, K. Yang, Research on superhydrophobic surface of biodegradable magnesium alloys used for vascular stents, Materials Science and Engineering C 33 (5) (2013) 2885–2890.
[35] S. Rokidi, P.G. Koutsoukos, Crystal Growth of Calcium Phosphates from Aqueous Solutions in the Presence of Strontium, Chemical Engineering Science 70 (2012) 3157–3164.
[36] F. Barrere, P. Layrolle, C.A. Van Blitterswijk, K. De Groot, Biomimetic calcium phosphate coatings on Ti6Al4V: A crystal growth study of octacalcium phosphate and inhibition by Mg^{2+} and HCO_3^-, Bone 25 (2) (1999) 107S–111S.
[37] F. Barrere, C. Van Blitterswijk, K. De Groot, P. Layrolle, Nucleation of biomimetic Ca–P coatings on Ti6Al4V from a SBF × 5 solution: influence of magnesium, Biomaterials 23 (10) (2002) 2211–2220.
[38] X. Lin, L. Tan, Q. Zhang, K. Yang, Z. Hu, J. Qiu and Y. Cai, The in vitro degradation process and biocompatibility of a ZK60 magnesium alloy with a forsterite-containing micro-arc oxidation coating, Acta Biomaterialia http://dx.doi.org/10.1016/j.actbio.2012.12.016, in press.
[39] J. Liang, P.B. Srinivasan, C. Blawert, W. Dietzel, Comparison of electrochemical corrosion behaviour of MgO and ZrO_2 coatings on AM50 magnesium alloy formed by plasma electrolytic oxidation, Corrosion Science 51 (10) (2009) 2483–2492.
[40] E. Boanini, P. Torricelli, M. Fini, A. Bigi, Osteopenic bone cell response to strontium-substituted hydroxyapatite, Journal of Materials Science: Materials in Medicine 22 (9) (2011) 2079–2088.
[41] A. Bigi, E. Boanini, C. Capuccini, M. Gazzano, Strontium-substituted hydroxyapatite nanocrystals, Inorganica Chimica Acta 360 (3) (2007) 1009–1016.